Structure and Activity of Two Photoreversible Cinnamates Bound to Chymotrypsin[†,‡]

Barry L. Stoddard,[§,∥] John Bruhnke,[⊥] Ned Porter,[⊥] Dagmar Ringe,[§,∥] and Gregory A. Petsko[*,§,∥]

Department of Chemistry, Massachusetts Institute of Technology, Cambridge, Massachusetts 02139, and Department of Chemistry, Duke University, Durham, North Carolina 27706

Received May 17, 1989; Revised Manuscript Received January 22, 1990

ABSTRACT: The serine protease γ-chymotrypsin was covalently inhibited with two different photoreversible cinnamate compounds, and the structures of the resulting complexes were determined to 1.9-Å resolution. The inhibitors show different kinetics of binding, inhibition, and nonphotochemical deacylation relative to each other in solution activity assays. The crystal structures of the enzyme–cinnamate complexes show that both compounds acylate serine 195 and that the two molecules are bound in similar nonproductive conformations which have drastic effects on their ability to turn over. Substitution of a diethylamino group on the para position of the cinnamate ring causes a 1000-fold increase in the thermal stability of the inhibitor toward hydrolysis and deacylation.

The structure and mechanism of γ-chymotrypsin and of the serine proteases in general are some of the most well-known and best understood in biochemistry. Chymotrypsin has been the target of a number of studies directed toward the development of novel mechanism-based inhibitors. One class of compounds that have been studied with great success has been a variety of dead-end inhibitors known as "suicide substrates" (Abeles & Maycock, 1976; Walsh, 1982). These compounds share the features of binding in a productive orientation for catalytic turnover and of possessing a latently reactive functional group that is activated during catalysis, leading to irreversible covalent modification of the enzyme by the inhibitor. One such compound is 3-benzyl-6-chloro-2-pyrone, a six-membered heterocyclic ring that acylates serine 195 and is bound to the enzyme via an ester linkage to the carbonyl carbon of the pyrone (Gelb & Abeles, 1984). X-ray diffraction analysis of the complex shows that upon binding the pyrone ring is opened, yielding a reactive C-5 carboxylate group that forms a salt bridge with the active site histidine (Ringe et al., 1986). Another example is inhibition by the benzoxazinones (Hedstrom et al., 1984), which produce upon binding an ortho-substituted benzoylchymotrypsin that deacylates slowly due to the electron-donating characteristics of the "released" substituent.

In contrast with compounds of the type mentioned above, other inhibitors of chymotrypsin have been studied that prevent catalysis through simple competitive acylation reactions to the active site serine. These compounds deacylate at a rate much reduced compared to that of substrate, implying that the energetic profile of the reaction is altered by the structure and binding of the inhibitor. Fluoromethyl ketones, for example, are bound as stable tetrahedral hemiketals and, in general, show reversible competitive inhibition (Imperiali & Abeles, 1986). The energetic barrier to deacylation is increased relative to that of unsubstituted peptide substrates due to the stabilization of the tetrahedral intermediate by the inductive effect of the fluorine atoms. In a much earlier study, it was shown that the rate of deacylation of benzoylchymotrypsin complexes can be dramatically affected by the substitution of specific groups (such as CH_3O–, Cl–, CF_3–, and NO_2–) on the phenyl ring of the leaving group, demonstrating the effect of differences in electronic properties between various substrates for altering the energetic profile of enzymatic turnover (Caplow & Jencks, 1962).

The inhibitors presented in this study are members of the latter family of competitive, reversible inhibitors. They are planar, aromatic compounds that bind specifically to chymotrypsin, acylate the active site serine, and have k_{cat}'s which are reduced by 4–5 orders of magnitude relative to those of peptide substrates. Unlike the compounds discussed above, however, these cinnamates possess the property of being converted by light of specific wavelengths from the trans geometric isomer into the cis form, which has a deacylation rate of 10^3–10^9-fold higher. This family of compounds is now under investigation as a possible class of light-activated therapeutic agents (Turner et al., 1987) and as possible chemical "triggers" for turnover in the protein crystal. It is hoped that such compounds will prove useful under a variety of experimental and physiological conditions.

With this goal in mind, two photoreversible cinnamate inhibitors specific for γ-chymotrypsin have been synthesized for the purpose of inhibiting the enzyme and then rapidly reactivating the inactive enzyme. We have solved the three-dimensional structures of the inhibited enzyme at 1.9 Å and measured the kinetics of binding, inhibition, and nonphotochemical deacylation of the inhibitor in solution. We are particularly interested in the mechanism of binding and inhibition for the compounds and the relationship between the energetic profile for deacylation mechanism and the structure of the E–I complex. In particular, we will concentrate on the basis for the enzymes' specificity toward these compounds, on the large difference in the rectivity of the cinnamates toward chymotrypsin compared to similar unconjugated phenyl ester

[†] This work was supported by NIH Grant HL-17921 to N.P. and NIH Grant GM26788 to G.A.P. and D.R. and by Payload Systems Inc. (G.A.P.).

[‡] Crystallographic coordinates have been submitted to the Brookhaven Protein Data Bank under 3GCH and 4GCH.

* Correspondence should be addressed to this author at his present address.

[§] Massachusetts Institute of Technology.

[∥] Present address: Rosensteil Center for Basic Medical Research, Room 650, Brandeis University, Waltham, MA 02254.

[⊥] Duke University.

0006-2960/90/0429-4871$02.50/0

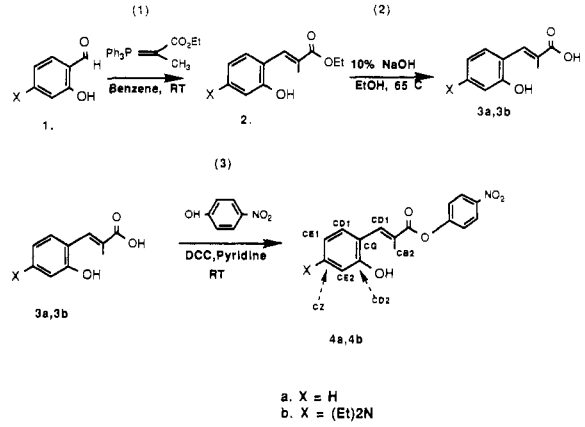

FIGURE 1: Synthetic pathway to cinnamates A and B.

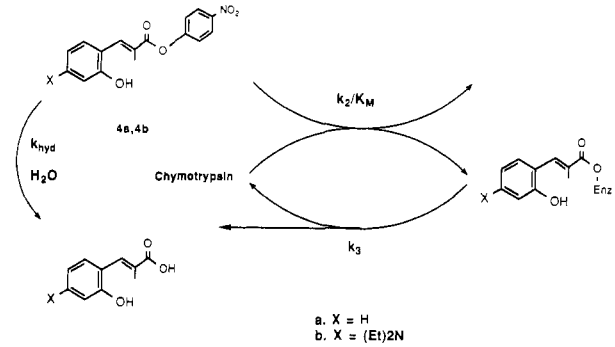

FIGURE 2: Kinetic pathway of nonphotochemical acylation and hydrolysis of chymotrypsin by cinnamates A and B.

substrate analogues, and on the difference in reactivity between the two compounds themselves. We hope to provide a reasonable overview of the inhibitory actions of photoreversible cinnamates so that we may then be in a position to examine and understand their ability to serve as light-induced chemical triggers. Our studies on the photochemical deacylation of the inhibitor from the enzyme in solution and in the crystal are presented in a separate paper.

Materials and Methods

Synthesis and Analysis of Photoreversible Cinnamate Inhibitors. Cinnamates A and B were synthesized in a three-step process from the initial materials *trans-o*-hydroxy-α-methylcinnamic acid (Turner et al., 1988), pyridine, and *p*-nitrophenol. The synthetic scheme for the preparation of the inhibitors used in this study is presented in Figure 1. Details for the synthesis and analytical data including NMR, UV, and elemental analysis for all compounds is presented as supplementary material (see paragraph at end of paper regarding supplementary material).

Solution Activity Assays of the Inhibitors. (*A*) *Reagents.* α-Chymotrypsin, type I-S, from bovine pancreas (lot 85F-8115) and bovine serum albumin (BSA) were purchased from Sigma Chemical Co., St. Louis, MO. Sephadex G-25 was purchased from Pharmacia Fine Chemicals, Piscataway, NJ. The chymotrypsin chromogenic substrate MeO-Suc-Arg-Pro-Tyr-*p*-nitroanilide hydrochloride, S-2586, was purchased from Helena Laboratories, Beaumont, TX. Tris Ultra Pure was purchased from Schwarz/MannBiotech, Cleveland, OH. All other reagents were of the finest commercial grade available.

(*B*) *Activity Assays.* The activity of α-chymotrypsin was determined by chromogenic assay using S-2586 (K_M = 32.6 μM, k_{cat} = 26.77 s^{-1}) in 30 mM Tris, 3 mM $CaCl_2$, and 400 mM NaCl, pH 8.3, at room temperature. In a typical assay, 150 μL of 1 mM S-2586 in H_2O was added to a solution of 20 μL of enzyme in 1000 μL of Tris buffer, pH 8.3, containing 1 mg/mL BSA. Enzyme concentrations were between 1 and 5 μM. The initial rate velocity was measured from the ΔA_{402} with time, which is then proportional to the change in concentration of active enzyme (Hemker, 1983; Lottenberg et al., 1981). Time courses of inhibition were conducted for various concentrations of inhibitors **4a** and **4b** with α-chymotrypsin. All experiments were conducted at room temperature in 50 mM Tris and 150 mM NaCl, pH 7.4, except for assays that were conducted in 30 mM Tris, 3 mM $CaCl_2$, and 400 mM NaCl, pH 8.3. Percent activity of α-chymotrypsin in the presence of inhibitor **4a** or **4b** was determined by chromogenic assay with S-2586.

To follow reactivation of inhibited enzyme in the absence of light, α-chymotrypsin was incubated (at room temperature) with 25 equiv of inhibitor for 6 h (Figure 2). For cinnamate B, the acyl-enzyme was then purified at room temperature on BSA-treated Sephadex G-25. The gel filtration procedure was performed on a 20 × 0.5 cm column. The return of enzyme activity was monitored by chromogenic assay, and a plot of $\ln [(E_\alpha - E_t)/(E_\alpha - E_0)]$ vs time subsequently yielded k_3, the rate constant for hydrolysis of the acyl-enzyme. The measured k_3 value and a simple numerical integration routine enabled us to curve fit the time course plots of inhibition to yield the second-order rate constant of inhibition (k_2/K_M). The cinnamate A–chymotrypsin complex, on the other hand, shows a much shorter half-life (Tables II and III), which made clean isolation of the acyl-enzyme in the time course of gel filtration impossible; therefore, k_2/K_m and k_3 for this inhibitor were determined by numerical-integration curve fitting. The uncatalyzed hydrolysis of the inhibitors was also measured independently, and the numerical integration was corrected for this background hydrolysis. Results of inhibitor kinetic assays are summarized in Table II. The product of deacylation (**3a** or **3b**) was identified by chromatography on silica gel.

Crystallization of γ-Chymotrypsin. A total of 300 mg of α-chymotrypsin (Sigma, C-4129) was dissolved into 2.5 mL of H_2O. Approximately 3 mL of aqueous potassium borate (0.5 M), pH 9.0 (boric acid adjusted with KOH), was added dropwise until the pH of the enzyme solution was 8.6. The sample was divided into 1-mL aliquots and incubated at 37 °C for 6 h. This step converts α- into γ-chymotrypsin [two forms of the enzyme that are covalently identical and almost indistinguishable in their folded conformations but differ in the way they crystallize, unfold in urea, and tend to dimerize—Cohen (1981) and Sharma et al. (1981)].

Solid ammonium sulfate was added to each aliquot until heavy precipitation was observed, and the tubes were allowed to sit at room temperature for 30 min. The samples were then centrifuged, and the supernatant was discarded. Each pellet was resuspended in 0.5 mL of H_2O, the aliquots were pooled, and the protein concentration for the sample was determined from A_{280} on a 1/100 dilution (A_{280} = 2.0 at 1 mg/mL). The solution was diluted to a final concentration of 15 mg/mL chymotrypsin in 10 mM sodium cacodylate (pH 5.6), 0.75% saturated cetyltrimethylammonium bromide, 45% saturated ammonium sulfate, and water to the final volume. The saturated ammonium sulfate solution must be added last to avoid irreversible precipitation of the enzyme.

This final solution was allowed to sit for exactly 1 h at room temperature and then passed through a 0.45-μm sterile filter to remove precipitated debris. Aliquots of 300 μL were then dispensed into the bottoms of open 0.5-dram vials, which were then placed into clear scintillation vials with a surrounding

reservoir of 1 mL of 65% saturated ammonium sulfate. The scintillation vials were sealed with screw caps and stored undisturbed for 2 weeks. Tetragonal crystals with symmetry $P4_22_12$, $a = b = 69.7$ Å and $c = 97.5$ Å, of size approximately 0.6 × 0.4 × 1.0 mm were routinely grown by this method.

Inhibition of γ-Chymotrypsin. Approximately 75 mg of each inhibitor was dissolved into 125 mL of fresh DMSO to make a stock solution of about 600 mg/mL (2.4 M). From the point of dissolution on, extreme care was taken that all steps involving the inhibitor were performed under a safe light. Four crystals of chymotrypsin were soaked for 60 days in 200 μL of 20 mM sodium cacodylate (pH 7.4) with 85% saturated ammonium sulfate and a 1/20 dilution of the inhibitor stock solution (10 μL of inhibitor). These soaking conditions provided approximately a 200:1 molar excess of inhibitor relative to protein in the drops. The concentration of inhibitor was approximately 120 mM. The soaks were agitated gently for 1 min to facilitate dispersion of the DMSO/inhibitor phase into the aqueous solution and then kept in total darkness at room temperature. The crystals became bright yellow during the soak, indicating reaction of the inhibitor with enzyme.

Binding of inhibitor was verified by backsoaking individual soaked crystals for 10 days against inhibitor-free mother liquor and then taking 24-h, 15° precession photos of the (*hk*0) zone, which were compared to similar photos of uninhibited specimens taken directly from the crystallization setups. Intensity changes were noticeable throughout the zone and were especially clear for the (0,18,0) and the (17,17,0) reflections. This is strong evidence that the inhibitor forms a stable covalent adduct to the enzyme in the crystall. For both inhibitors the crystals were isomorphous with native chymotrypsin to within 0.2 Å on all three unit-cell axes.

Data Collection. After 2 months the crystals were mounted in quartz capillaries (0.7–2.0-mm inner diameter, Charles Supper Co.). The capillaries contained a small volume of mother liquor at one end to prevent desiccation of the crystal and were sealed at both ends with mineral oil, wax, and petrolatum. For the initial data collection, two crystals were used for each inhibitor to give a complete data set to 1.9-Å resolution. Data were collected in the dark at 20 °C on a Nicolet four-circle diffractometer with a sealed-tube X-ray generator running at 45 kV, 35 mA. All data were collected with an ω scan, and individual background measurements were taken for each reflection. Corrections for absorption by the specimen were made by collecting absorbance curves over 360° on φ; reflection intensities were measured every 15° for the same reflection, and the resulting curve was used to correct the entire data set. Such effects were observed to be negligible due to the uniform shape of the crystals and small segment of reciprocal space needed for data collection of tetragonal crystals (45°). Five standard reflections were remeasured for each 300 measurements to monitor and correct for radiation decay; the individual decay curves were in all cases extremely linear (95% or higher correlation to a least-squares fit). No crystal experienced more than 40% decay over the total extent of data collection. Friedel pairs were not collected due to the high quality of the data (5% merging and symmetry-related R factors, mean F/σ ratio of 5.0). The structures were built and analyzed by the FRODO program of Dr. Alwyn Jones on an Evans and Sutherland PS300 graphics system (Jones, 1978), using initial chymotrypsin coordinates taken from the Brookhaven Protein Data Bank for the structure of uncomplexed γ-chymotrypsin (Cohen et al., 1981). The initial maps were calculated as $2F_o - F_c$ Fourier difference maps with calculated F's and phases derived from the PDB structure. No inhibitor coordinates were included in the Fourier synthesis. For both structures the initial maps clearly showed the inhibitors bound in the active site.

The inhibitors were built into the maps, and the two structures were refined from the initial coordinates by the restrained least-squares method (PROLSQ) on a Vax 11/750 (Konnert & Hendrickson, 1980). The refinements were completely independent of one another except for the use of the same starting coordinates. The serine γ-oxygen to cinnamate carboxyl oxygen distance was held constant at 1.5 Å during the refinement, and the bond angle was left unrestrained.

The Babinet correction was used to aid in the refinement of low-resolution data (Fraser et al., 1978), and individual atomic thermal factors were used in the last stages of both refinements. Detailed information for each data set collected is presented in Table I.

Table I: Summary of Data Sets and Refined Structures

	cinnamate A	cinnamate B
resolution (Å)	50–1.9	45–1.9
no. of reflections	9635	10856
low-intensity cutoff	2σ	2σ
no. of crystals per data set	2	2
crystals 1 and 2 merging overlap (F's)	742	247
merging R factor (F's) (%)	5.0	5.2
mean F/σ ratio	5.5	4.5
total non-hydrogen atoms	1824	1826
total waters in final structure	73	70
initial overall R (%)[a]	43.6	40.2
final overall R (%)	20.3	20.9
total distances (Å)	6017	6160
total nonideal distances (Å)[b]	649	690
bond dist RMS/σ	0.018/0.020	0.021/0.020
planar group RMS/σ	0.026/0.025	0.026/0.025
chiral center RMS/σ	0.221/0.150	0.238/0.150
nonbonded contact RMS/σ		
single torsion	0.215/0.500	0.237/0.500
multiple torsion	0.309/0.500	0.315/0.500

[a] $R = \sum(F_o - F_c)/\sum F_o$. [b] Distances deviating by more than 0.04 Å from their ideal van der Waals contact distances.

Table II: Inhibition of Chymotrypsin by Cinnamates A and B

inhibitor	k_2/K_M (M^{-1} s^{-1}) (acylation)	k_3 (s^{-1}) (enzymatic hydrolysis)	k_{hyd} (s^{-1}) (nonenzymatic hydrolysis)
4a (R = H)	1.1×10^4	1.3×10^{-3}	4.4×10^{-6}
4b (R = Et_2N)	4.5×10^1	2.4×10^{-6}	4.9×10^{-5}

RESULTS

(*A*) *In Vitro Studies of Inhibitor Binding and Activity.* The rates of acylation, deacylation, and nonenzymatic hydrolysis of inhibitors A and B have been measured as described under Materials and Methods and are summarized in Table II. Cinnamate A (nonsubstituted) shows a significant reduction of approximately 5 orders of magnitude in reactivity relative to similar phenyl substrates reported in the literature (see Table III), which can be explained in terms of the structure of the enzyme–inhibitor complex and the interactions of the conjugated, planar compound with the well-categorized transition-state stabilizing ligands of the enzyme (see Discussion).

Cinnamate B was synthesized in order to increase the efficiency and rate of photoisomerization when bound to the enzyme. As can be seen in the reactivity of the two inhibitors relative to one another, this para-substituted inhibitor (**4b**) is approximately 3 orders of magnitude less reactive to acyl attack by serine 195 of the active enzyme and to hydrolysis of the inhibited E–I complex.

Table III: Deacylation Rates of Phenyl Substrates vs Methylcinnamate Ester

substrate	structure	k_3 (s^{-1})	reference
benzoate (acetyl ester)	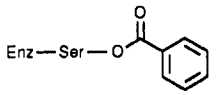	2.05×10^2	Caplow & Jencks, 1962
N-acetyltyrosine (nitrophenyl ester)	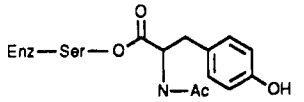	2.0×10^2	Zerner et al., 1971
N-acetylphenylalanine (nitrophenyl ester)	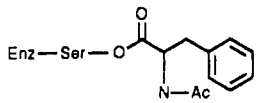	7.7×10^1	Berezin et al., 1964
o-hydroxymethylcinnamate (nitrophenyl ester)	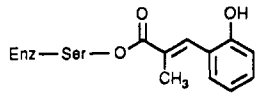	1×10^{-3}	Table II

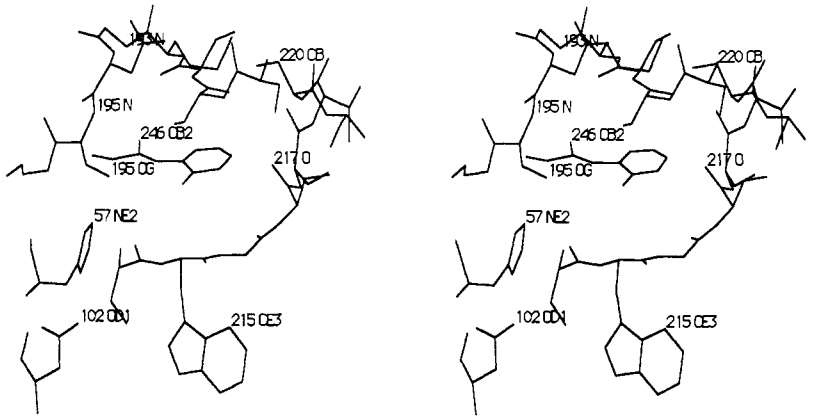

FIGURE 3: Stereo diagram of cinnamate A bound to chymotrypsin. Visible are members of catalytic triad (Asp 102, His 57, and Ser 195), the cinnamate inhibitor, and the regions of peptide (residues 190–196 and 214–220) that flank the specificity pocket and serve to restrain the bound inhibitor in a rigid planar conformation (see Table IV for interatomic distances).

(B) Crystallographic Studies of Inhibitor Binding. The two inhibitors both show clear covalent binding to serine 195 in the active site. They differ in a subtle manner, however, in the conformation, contacts, and interactions that exist in the enzyme–inhibitor complex. These two structures shed a great deal of light on the relative activity of the two compounds as photoreversible inhibitors in vitro and also offer some insight into the function of competitive enzymatic inhibitors in general.

(1) Binding of p-Nitrophenyl o-Hydroxy-α-methylcinnamate (Cinnamate "A"—No Amino Substituent Present). The inhibitor is bound as a completely planar 12-atom molecule in the active site of the enzyme (Figures 3 and 6). The acyl bond from the γ-oxygen of serine 195 to the inhibitor carboxyl oxygen is 1.5 Å long and refines to a bond angle of 120°. The bonds to the carbon describe a planar group consistent with an sp^2-hybridized acyl intermediate. The carbonyl oxygen lies in the plane of the inhibitor structure and clearly points away from backbone nitrogens 193 and 195 of the oxyanion hole, which are located almost 5 Å from the inhibitor oxygen; its nearest nonbound neighbors are instead CB and CA 195 with interatomic distances of 1.87 and 3.17 Å.

The phenyl ring is found in the P_1 side-chain binding site and is surrounded on both faces by atoms of the peptide backbone, with the closest contacts to the ring consisting of atoms from residues 190–195 and 213–217. These two stretches of peptide flank the opposite sides of the phenyl ring, forming a hydrophobic cleft that accommodates the aromatic structure of the inhibitor and serves to anchor the cinnamate in place. Numerous van der Waals contacts between the π electron clouds of the conjugated ring and the main-chain nitrogen and carbonyl groups of the backbone are observed, with interatomic distances of 3.1–3.9 Å from the protein chain to the aromatic carbons of the inhibitor. These contacts exist almost exclusively at an angle close to perpendicular to the plane of the phenyl ring, forming polar interactions between the π electron clouds of the inhibitor and the backbone atoms of the specificity pocket. Such interactions are well docu-

Table IV: Closest Atomic Contacts and Distances for Cinnamate A Structure[a,b]

	neighbor				neighbor		
inhibitor	residue	atom	distance (Å)	inhibitor	residue	atom	distance (Å)
O	195	OG	2.43	CE1	217	O	3.15
	57	NE2	2.84		192	SD	3.61
	195	CA	3.17	CE2	216	N	3.60
C	195	OG	1.54		215	C	3.78
	195	CB	1.95		216	C	3.95
	57	NE2	3.10		217	O	3.91
	214	O	3.86	CZ	217	O	2.69
CA	195	OG	2.00		217	C	3.78
	214	O	3.97		216	O	3.81
CB1	191	O	3.68		216	C	3.80
	214	O	3.77		220	SG	3.98
CB2	192	CA	3.96	OH	215	O	3.50
GG	191	O	3.95		215	N	3.61
CD1	192	SD	3.85		215	C	3.42
	192	N	3.89	N	217	O	1.89
CD2	215	C	3.61				
	215	CA	3.71				
	216	N	3.86				

[a] Distance from O-217 to the inhibitor nitrogen is for cinnamate B. [b] The labeling of the inhibitor atoms is illustrated in Figure 1.

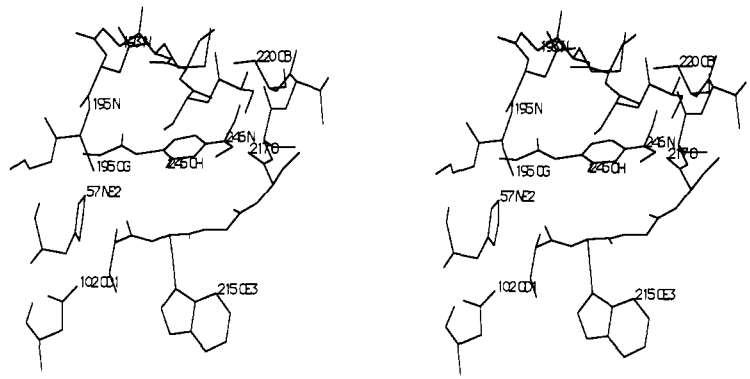

FIGURE 4: Stereo diagram of cinnamate B bound to chymotrypsin. The same groups of the active site are shown as in Figure 3.

mented (Burley & Petsko, 1985; Singh & Thornton, 1985) and can provide large contributions to the binding and stabilization of aromatic ligands by proteins. Table IV shows the nearest neighbors to all atoms of cinnamate A with the corresponding interatomic distances.

The hydroxyl oxygen of the ring also is within hydrogen-bonding distance of the backbone carbonyl oxygen of residue 215. The contacts of the inhibitor phenyl ring appear to provide the largest contribution to the orientation of the inhibitor in the active site. Due to the planarity of the molecule and the binding of the cinnamate in the specificity pocket, the inhibitor is observed to bind in a nonproductive conformation such that the carbonyl oxygen of the cinnamate is not found in the "oxyanion hole", where electrostatic interactions with the oxygen would stabilize the tetrahedral intermediate normally formed during successful catalysis or hydrolysis.

Histidine 57 is in close proximity to the nucleophilic serine [3.3 Å between Ser 195 (Oγ) and His 57 (Nϵ_2)] and shares a clear hydrogen bond with aspartate 102 via His 57 (Nθ_1). Thus, the histidine has extracted a proton, as expected, and can participate in general-acid/general-base catalysis through the charge-relay system. The protonated nitrogen of His 57 (Nϵ_2) lies in close proximity to the acyl oxygen of the cinnamate. Because of the binding of the planar inhibitor, the acyl oxygen is actually found close to where the nitrogen of an amide substrate would be found before proton transfer by the histidine during turnover (Steitz & Shulman, 1982).

The binding pocket appears devoid of bound water molecules with the exception of one molecule interacting tightly with the β-carbon of the inhibitor and several atoms of the specificity pocket peptide chain. The structure refined to an *R* factor of 20.3% with good geometry, and 73 water molecules were assigned explicitly per enzyme monomer. Comparison of the structure with the original structure for γ-chymotrypsin as reported by Davies et al. gives an RMS deviation of 0.49 Å for all atoms and 0.28 Å for α-carbons. Of the residues of the active site and the specificity pocket, serine 195 shows the largest motion upon binding of the cinnamate, with Cα shifted by 0.4 Å. None of the other residues mentioned above, including His 57 and Asp 102, deviate significantly from their positions in the initial structure.

(2) *Binding of p-Nitrophenyl o-Hydroxy-p-(diethylamino)-α-methylcinnamate (Cinnamate "B"—with Diethylamino Group on Phenyl Ring).* This inhibitor also acylates serine 195 (Figures 4 and 7) and binds as a completely planar molecule (with the exception of the sp^3 carbons of the diethylamino substituent). The serine to cinnamate carbonyl bond length is approximately 1.5 Å. The compound is found in the same orientation as cinnamate A with the phenyl ring located in the hydrophobic specificity pocket described above. The carbons of the diethylamino group appear to experience steric crowding against the backbone atoms of residues 217–219. These interactions result in a shift of the entire inhibitor toward serine of approximately 0.85 Å (a shift of 0.83 and 0.85 Å for Cα and Cβ_1 of the inhibitor is observed) and a rigid-body rotation of the molecule of about 5° in the binding pocket. The active site residues appear to accommodate this movement of the molecule with minimum rearrangement, relying primarily on a torsion angle rotation of approximately 45° about the serine 195 Cα–Cβ bond, which results in a movement of the serine γ-oxygen of approximately 0.85 Å. The α-carbons of residues 212–215 have shifted away from the inhibitor by an average of 0.42 Å, resulting in a correspondingly wider binding pocket. The two cinnamate-bound structures differ from one another by an RMS of 0.20 Å between corresponding α-carbons. The amino nitrogen of the inhibitor appears to show a weak interaction with the backbone carbonyl oxygen of residue 217, with a measured distance of 1.89 Å for the refined structure. Such an interaction may to a small degree explain the increased thermal stability of the acyl-enzyme compared to that of the previous structure. The carbonyl oxygen is found in the same conformation as that in the first inhibitor—in the plane of the inhibitor structure and pointing away from the oxyanion hole. Figure 5 shows the two inhibitors superimposed on one another in their respective orientations in the active site.

The electron density for the *o*-hydroxyl group and the *p*-amino nitrogen as well as for the first two substituent carbons are extremely clear and well formed; in contrast, the density for the terminal carbons of the aminoethyl chains is weaker, implying more torsional disorder for those atoms. The distance and identity of nearest atomic contacts to the inhibitor are comparable to those of cinnamate A.

Discussion

This paper describes the structures and biochemistry of a pair of photoreversible inhibitors of chymotrypsin intended to serve as chemical "triggers" for enzymatic catalysis. In order to perform time-resolved structural studies of enzymatic intermediates, our starting base of knowledge of the system must be as complete and well understood as possible, in order to have any chance of obtaining interpretable results. Chymotrypsin offers some advantages in this regard:

(1) The enzyme mechanism is well categorized energetically and kinetically. Studies of rate constants for acylation, hydrolysis, and catalysis, as well as accurate binding constants for scores of substrates and inhibitors (Hein & Niemann, 1962a,b; Caplow & Jencks, 1962; Zerner, 1964; Berezin, 1971; Fersht, 1977), have made the mechanism of catalysis by chymotrypsin one of the best understood in the field.

(2) The three-dimensional atomic structure of chymotrypsin (with a bound inhibitor) has been solved and refined to ex-

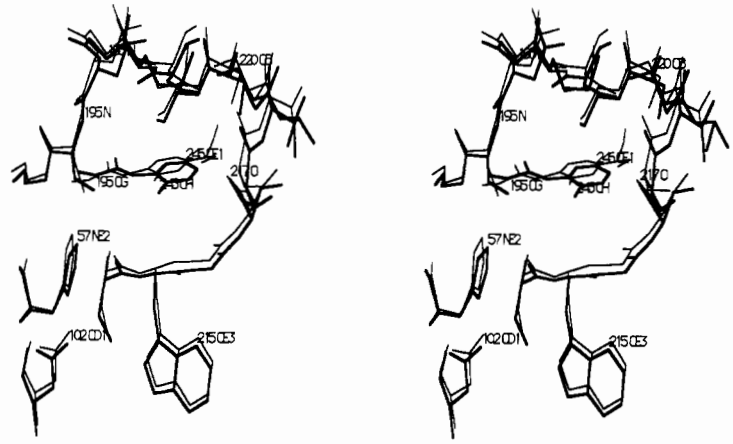

FIGURE 5: Stereo diagram with the cinnamate inhibitors superimposed in the orientations in which they are found in the active site. Heavy bond lines are the cinnamate A complex; light bond lines are cinnamate B. The same atoms are shown as in Figures 3 and 4.

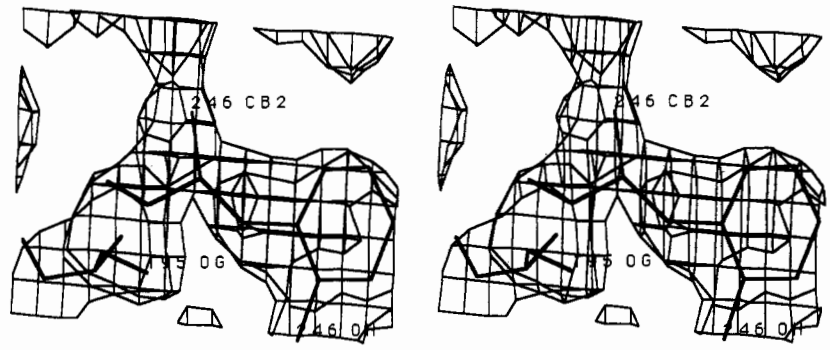

FIGURE 6: Stereo diagram of cinnamate A electron density in the active site of chymotrypsin with atomic model included. Inhibitor is viewed perpendicular to the plane of the conjugated phenyl ring. Map was calculated as a $2F_o - F_c$ Fourier synthesis at 2.2-Å resolution with the cinnamate deleted from the calculation.

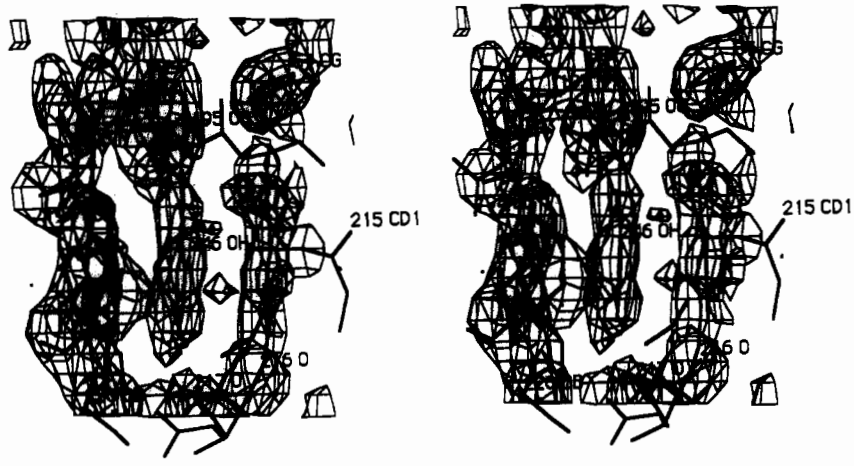

FIGURE 7: Structure of cinnamate A bound in the active site of γ-chymotrypsin. The inhibitor, viewed here edge-on in the center of the figure with the phenyl hydroxyl group pointing out of the page, is covalently bound to serine 195, which is found directly above the inhibitor. His 57 is visiable in the upper-right quadrant of the figure. The ring of the inhibitor is flanked by residues 191–194 on the left and residues 214–217 on the right. These two stretches of peptide provide the bulk of the binding interactions to the cinnamate. Note the rigid planarity of the entire molecule within the specificity pocket. Nitrogens 193 and 195 of the oxyanion hole are visible on the upper-left peptide chain flanking the bound inhibitor and are not capable of binding the cinnamate acyl oxygen without free rotation about the α-carbon of the inhibitor. The figure is a 2.2-Å $2F_o - F_c$ Fourier synthesis with the cinnamate and serine 195 deleted from the phase calculation.

tremely high (1.5 Å) resolution (Ringe et al., 1985). The identity and importance of the residues that play a role in the binding and turnover of substrate are therefore also quite well-known and understood. From this knowledge, reasonable deductions may be made about the actions of inhibitors such as the ones in this work.

The work detailed in this paper on these inhibitors sheds interesting light on the mechanism of serine proteases in general and on the challenge of rationally designing any mechanism-based enzyme inhibitor. Our most important observations relate to the binding of these inhibitors in the enzyme active site and to their reactivity with chymotrypsin compared to that with one another and with other well-categorized compounds.

Binding of the Cinnamate and Role of Planarity and Resonance for Inhibition. As mentioned earlier, both inhibitors acylate serine 195 and are bound as completely planar molecules with the phenyl ring buried in the specificity pocket.

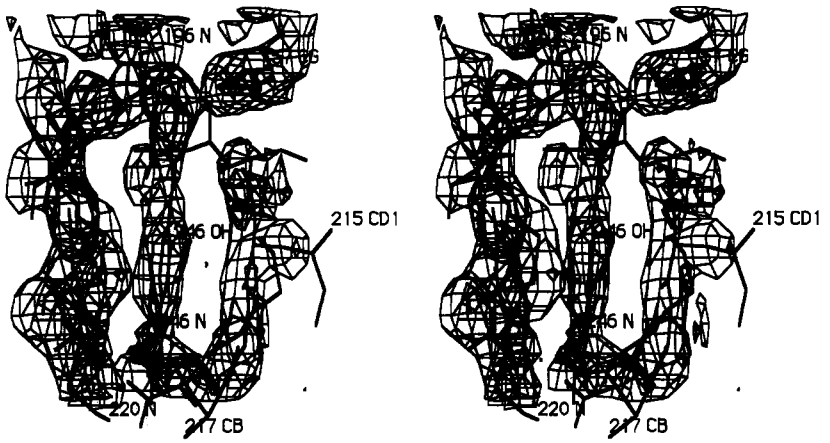

FIGURE 8: Structure of cinnamate B bound in the active site of γ-chymotrypsin. This inhibitor, viewed here in the same orientation as for Figure 7, is also covalently bound to serine 195. Extra density for the *p*-(diethylamino) group is clearly present, and the trigonal, planar shape of the conjugated nitrogen is visible. This molecule is bound in a rigid planar configuration similar to cinnamate A but is shifted toward residues 195 and 196 by approximately 0.85 Å and rotated by 5°. This translation in the inhibitor orientation is accommodated by a 45° bond rotation between Ser Cα Ser Cβ and a corresponding movement by Ser Oγ by 0.85 Å relative to the cinnamate A structure (see Figure 5). The surrounding peptide backbone has shifted very little in order to accommodate the larger inhibitor structure (see Discussion). The figure is a $2F_o - F_c$ Fourier synthesis with the cinnamate and serine 195 deleted from the phase calculation.

Numerous binding interactions between the phenyl ring and protein backbone appear to dictate the overall orientation of the compound in the active site. The lack of rotational freedom about the bonds of the cinnamate sp^2 α-carbon compared to similarly bound substrate residues causes the acyl oxygen clearly to point away from the oxyanion hole, preventing proper stabilization of the tetrahedral intermediate during hydrolysis. The magnitude of this effect is illustrated by the deacylation rates presented in Table III for cinnamate A as compared to two similar *N*-acetyl amino acid substrates. These substrates show a deacylation rate of approximately 10^2 s^{-1}, as compared to a rate of 10^{-3} for the *o*-hydroxylcinnamate (a decrease of 5 orders of magnitude).

In addition to this steric effect of the double bond α to the carbonyl in hindering transition-state stabilization, there is the possibility of a deactivating electronic effect at the carbonyl carbon due to increased electronegativity caused by resonance of the uncharged inhibitor. This can be a very strong effect, as can be seen from the rates of acylation and deacylation for *p*-amino-substituted cinnamate B (see below). For unsubstituted cinnamate A, such resonance effects would entail delocalizing a positive charge over the carbons of the phenyl ring and the β-carbon. These resonance contributors probably provide a minimal percentage of the structural and charge characteristics of the inhibitor due to this unfavorable charge splitting. This is especially apparent when one compares the deacylation rate of the conjugated benzoate ester–enzyme complex (Table III) with the deacylation rates of the methylcinnamate complex. The rate for the benzoate acyl-enzyme appears to be unaffected by the conjugation of the phenyl ring to the carbonyl group, leading us to conclude that the primary reason for the inhibitory properties of unsubstituted cinnamate A is the formation of an unproductive geometry upon acylation of the enzyme.

It has been pointed out by one of the referees that the deacylation rate shown in Table III for the benzoate complex is for an imidazole *amide* substrate (as opposed to the nitrophenyl *ester* substrates used to illustrate the effect of rotational freedom on deacylation), implying that these rates are not truly comparable, since such substrates have opposite rate-limiting steps. In this case, however, the rate reported for the benzoate is the directly measured rate of deacylation for the isolated and purified acyl-enzyme [p 884 of Caplow and Jencks (1962)], whereas for the nitrophenyl ester substrates the rate shown in Table III is the k_{cat} for two species for which the rate-limiting step has been shown to be deacylation (Zerner et al., 1971; Berezin et al., 1964). Therefore, the values shown in Table III all show the quantitative value of the rate of deacylation for various chymotrypsin substrates. What is clear from this comparison is that, for acylated chymotrypsin, the rate of regeneration of free enzyme is highly dependent on subtle differences in the structure, geometry, and torsional freedom of the bound species after acylation.

The total effect of the nonproductive orientation of cinnamate A and of any small resonance deactivation of the carbonyl can be measured quite easily by examining the rates of acyl-enzyme deacylation of the compounds reported in Table III. The rate of deacylation for the nonplanar *N*-acetylphenylalanine and -tyrosine substrates can be estimated at roughly 1×10^2 s^{-1}[8] as compared to a measured rate of deacylation of 1×10^{-3} s^{-1} for cinnamate A (no amino substituent)—a difference of 5 orders of magnitude.

Using the simple relationship between any rate constant and the corresponding free energy of activation for that chemical step (Walsh, 1979), we can calculate what this difference in rates means in terms of the energy barrier to deacylation:

$$k_{obs} = (RT/nh)\exp(-\Delta G^{\ddagger}/RT)$$

$$\frac{k(1)}{k(2)} = \frac{(RT/nh)\exp[-\Delta G(1)^{\ddagger}/RT]}{(RT/nh)\exp[-\Delta G(2)^{\ddagger}/RT]} = \frac{\exp[-\Delta G(1)^{\ddagger}/RT]}{\exp[-\Delta G(2)^{\ddagger}/RT]} = \exp[-\Delta G(1)^{\ddagger}/RT + \Delta G(2)^{\ddagger}/RT]$$

$$\ln\frac{k(1)}{k(2)} = \frac{\Delta G(2)^{\ddagger} - \Delta G(1)^{\ddagger}}{RT}$$

If the rates of deacylation $k(1)$ and $k(2)$ are 10^2 and 10^{-3} s^{-1}, respectively, for unconjugated benzoyl substrates and for *trans*-α-methylcinnamate, then the difference in $\Delta G^{\ddagger}$ works out to approximately 7 kcal/mol—an impressive difference in energy barriers. If we ascribe this difference in deacylation rates primarily to the planarity of the cinnamate preventing proper transition-state stabilization of the tetrahedral carboxyl anion by the oxyanion hole during hydrolysis, then the difference in deacylation rates could stem from one of two possible sources: either the carbonyl oxygen is incapable of

swinging into the oxyanion hole altogether, causing a destabilized or partially stabilized negative charge on the transition state; or possibly the carbonyl oxygen does move into a productive conformation but only at a large energetic cost, leading to increased thermal stability over previously reported substrate analogues and a trapped intermediate species. A value of 7 kcal/mol is quite reasonable for a pair of hydrogen bonds between a charged oxygen and two protonated, partially charged nitrogens (N-193 and -195 of the oxyanion hole). The value for such an interaction in an aqueous environment can range from 3 to 5 kcal/mol per H-bond, depending on the polarity of the environment and on the distance between the atoms (Creighton, 1984; Burley & Petsko, 1986).

When considering the geometric effects of binding and the relationship of geometric requirements to catalysis, we should remember that we are considering a two-state problem, where the two states are bound acyl-enzyme of cinnamate A and the corresponding transition state for its deacylation, as compared to the bound state of a model substrate such as *N*-acetyltyrosine and its corresponding transition state for hydrolysis. Cinnamate A is bound in an unproductive orientation that cannot readily attain the enzymatically stabilized geometry of the transition state, whereas the model compounds are bound in a productive arrangement that can lead to the transition state with minimum reorganization.

These findings are in agreement with the structure of the acyl-enzyme (indolylacryloyl)chymotrypsin (Henderson, 1970), where the carbonyl oxygen is not productively bound but rather is bound via a bridging water molecule to the catalytic nitrogen atom of His 57. As Henderson and later Fersht (1977) state, the carbonyl oxygen must swing into the oxyanion hole for deacylation to occur, and proper binding of the amino group and the aromatic ring of the substrate is required for the carbonyl group to bind in such a productive mode. If either of the anchors is missing, the carbonyl binds in a nonproductive orientation.

An interesting point about these inhibitors is the fact that acylation occurs at all given the constrained geometry of the compound and its inability to achieve proper transition-state stabilization during deacylation. Either binding occurs with the proper conformational change in the inhibitor and stabilization of the carboxyanion, or else the differences in nucleophile and leaving-group species between acylation and deacylation are sufficient to cause a substantial difference in the rates of the two steps. It has been observed that cinnamates with various leaving groups at the nitrophenyl position differ significantly in their reactivity to chymotrypsin and other serine proteases; this is due to differences in their stability as leaving groups and also to their ability to bind specifically to the enzyme. As outlined by Hein and Neimann (1962), the binding energy derived by interactions of the leaving group in the P_3 site should contribute to the rate of acylation for the enzyme. It has also been shown that the nature of the leaving group can directly effect the identity of the rate-determining step of turnover for chymotrypsin (Zerner et al., 1964). What is clear is that proximity effects in the active site appear to be capable of overcoming steric and electronic hindrance in the binding of inhibitor.

Effect of Resonance on the Reactivity of Cinnamates A and B. The rate constants for binding and deacylation are substantially reduced for *p*-amino-substituted cinnamate B, which was originally synthesized in order to increase the photoefficiency of the light-driven isomerization. As shown in Table II, the substituted cinnamate B acylates chymotrypsin 250 times slower and deacylates 500 times slower than the same compound without the para-substituted diethylamino group attached to the phenyl ring. This effect must derive from one of two possible sources: steric effects in the active site (due to difficulty in accommodating the bulky amino group) and/or electronic resonance effects.

The structures of the two acyl-enzymes clearly show that the active site of chymotrypsin and the backbone of the specificity pocket have to "open up" somewhat in order to accommodate the larger cinnamate. The serine 195 γ-oxygen, along with the bound inhibitor, is pulled back from the specificity pocket approximately 0.85 Å to facilitate binding, and the specificity pocket is measurably wider. The electron density of cinnamate B also argues that, in forcing the binding pocket to open slightly, the inhibitor has given itself extra room for torsional movement about the acyl bond to the serine.

Such rearrangements of the enzyme active site, however, cannot reasonably be expected alone to cause a large difference in rate constants (as the very small differences in deacylation rates between benzoylchymotrypsin and *N*-acetylphenylalanine chymotrypsin show). Something else must contribute to the difference in reactivity between the two cinnamates. A reasonable explanation is provided by resonance.

Aside from the structure of (diethylamino)cinnamate shown in Figure 1, an alternative resonance form exists:

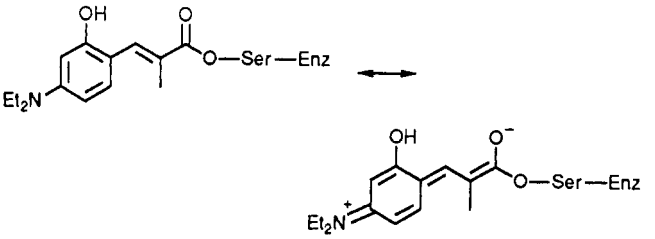

The second resonance contributor should be a major contributor to the structure of the inhibitor due to the presence of the very stable iminium cation (also seen in the H-bonded aldimine form of PLP). This should reduce the rate of deacylation significantly due to the increased electron density on the carbonyl rising from the contribution of nonelectrophilic enolate ion in the structure. A good Hammett correlation for the deacylation rate has been observed with several substituted cinnamates and factor Xa, and the reactivity difference between the H and diethylamino structures is maintained for several serine proteases under examination (Ned Porter, private communication). The planar, roughly trigonal electron density of the nitrogen of cinnamate B supports the existence of considerable double-bonded character in the *p*-amino group.

This work illustrates the importance of electronic and geometric considerations in the rational design of chemical agents that are intended to interact with proteins in order to affect their function. We have described the importance of transition-state stabilization for the specific case of a serine protease and shown that compounds such as these cinnamates illustrate a potentially important method of inhibiting enzymatic function, namely, by the use of one source of binding energy (phenyl ring interactions in specificity pocket) along with a geometric constraint (planar double bond) in order to prevent the formation of another binding interaction (tetrahedral oxyanion stabilization) which is essential for catalysis. In the specific case of serine proteases, molecules designed to bind with appropriate specificity, but with a carbonyl oxygen which cannot go into the oxyanion hole, should provide a fertile source of specific serine protease inhibitors.

In conclusion, this paper attempts to describe in some detail the chemistry of binding and deacylation of two possible photoreversible cinnamate inhibitors of chymotrypsin. Such

a study is necessary in order to use such compounds as tools in the construction of an enzymatic system for observing intermediates in catalysis. Work has also been done on measuring the rate of photolysis in solution and in the crystal for both inhibitors as the second step in designing a successful Laue experiment. Results of this work (the "light" reactions of these inhibitors with chymotrypsin) are reported in the next paper of this series, with consideration given to photochemical design and the use of an effective chemical trigger.

ACKNOWLEDGMENTS

We acknowledge the invaluable assistance and advice of Jeff Guynn, Dr. Gregory K. Farber, Steven C. Almo, and Dr. Barbara Seaton-Head. B.L.S. is supported by a Whitaker College Health Fund Fellowship. Thanks to Dr. Alex Rich for the use of his diffractometer for data collection.

SUPPLEMENTARY MATERIAL AVAILABLE

Syntheses and analyses of photoreversible cinnamate inhibitors **4a**, **2**, **3b**, and **4b** (3 pages). Ordering information is given on any current masthead page.

REFERENCES

Abeles, R. H., & Maycock, A. L. (1976) *Acc. Chem. Res. 9*, 313–319.

Berezin, I. V., Kazanskaya, N. F., & Klyosov, A. A. (1971) *FEBS Lett. 15*, 121.

Burley, S. K., & Petsko, G. A. (1985) *Science 229*, 23.

Caplow, M., & Jencks, W. P. (1962) *Biochemistry 1*, 883–893.

Cohen, G. H., Silverton, E. W., & Davies, D. R. (1981) *J. Mol. Biol. 148*, 449–479.

Creighton, T. E. (1984) *Proteins: Structures and Molecular Properties*, pp 133–152, Freeman, New York.

Fersht, A. (1977) *Enzyme Structure and Mechanism*, Freeman, New York.

Fraser, R. D. B., MacRae, T. P., & Suzuki, E. (1978) *J. Appl. Crystallogr. 11*, 693–694.

Gelb, M. H., & Abeles, R. H. (1984) *Biochemistry 23*, 6596–6604.

Hedstrom, L., Moorman, A. K., Dobbs, J., & Abeles, R. H. (1984) *Biochemistry 23*, 1753–1759.

Hein, G. E., & Niemann, C. (1962a) *J. Am. Chem. Soc. 84*, 4487–4494.

Hein, G. E., & Niemann, C. (1962b) *J. Am. Chem. Soc. 84*, 4495–4503.

Hemker, H. C. (1983) *Handbook of Synthetic Substrates for the Coagulation and Fibrinolytic System*, Nijhoff Publishers, Boston.

Henderson, J. (1970) *J. Mol. Biol. 54*, 341.

Imperiali, B., & Abeles, R. H. (1986) *Biochemistry 25*, 3760–3767.

Jones, T. A. (1978) *J. Appl. Crystallallogr. 11*, 268–272.

Konnert, J. H., & Hendrickson, W. A. (1980) *Acta Crystallogr. A36*, 344–350.

Lottenberg, R., Christensen, U., Jackson, C. M., & Coleman, P. L. (1981) *Methods Enzymol. 80*, 341–361.

Ringe, D., Seaton, B. A., Gelb, M. H., & Abeles, R. H. (1985) *Biochemistry 24*, 64–68.

Ringe, D., Mottonen, J. M., Gelb, M. H., & Abeles, R. H. (1986) *Biochemistry 25*, 5633–5638.

Sharma, S. K., & Hopkins, T. R. (1981) *Bioorg. Chem. 10*, 357–374.

Singh, J., & Thornton, J. M. (1985) *FEBS Lett. 190*, 1.

Steitz, T. A., & Shulman, R. G. (1982) *Annu. Rev. Biophys. Bioeng. 11*, 419–444.

Turner, A. D., Pizzo, S. V., Rozakis, G., & Porter, N. A. (1987) *J. Am. Chem. Soc. 109*, 1274–1275.

Turner, A. D., Pizzo, S. V., Rozakis, G., & Porter, N. A. (1988) *J. Am. Chem. Soc. 110*, 244.

Walsh, C. T. (1979) *Enzymatic Reaction Mechanisms*, p 32, Freeman, New York.

Walsh, C. T. (1982) *Tetrahedron 38*, 871–909.

Zerner, B., Bond, R. P. M., & Bender, M. L. (1964) *J. Am. Chem. Soc. 86*, 3674.